Proc. of the IEEE Global Telecommunications Conference GLOBECOM 2000, San Francisco, CA, USA, pp. 1488-1493, Nov. 2000.

Comparison of Preamble Structures for Burst Frequency Synchronization

Stefan H. Müller–Weinfurtner

Lehrstuhl für Nachrichtentechnik II, Universität Erlangen–Nürnberg, D–91058 Erlangen, Germany
http://www.LNT.de/LNT2/

Abstract— **Two types of repetition preambles are compared concerning frequency synchronization in burst transmission. A near–optimum frequency estimation algorithm with scalable lock–in range is proposed in conjunction with a reduced–overhead synchronization preamble, the so–called sandamble. Even though the fundamental ideas are independent from the specific modulation scheme, we study the algorithms in an Orthogonal Frequency–Division Multiplexing (OFDM) system.**

Keywords— **Preamble Design, Sandamble, Frequency Synchronization, OFDM**

I. Introduction

BURSTY transmission requires reliable single–shot synchronization. Further, training–data overhead for frame and frequency synchronization should be low. For this purpose, preamble schemes with periodic signal repetitions [1], [2] are often used. Such repeated signal structures allow coarse frame synchronization by finding the extremum of appropriate metrics [3], [4]. A frequency offset estimate is obtained from correlation results.

By variation of the size of repeated signal segments and their mutual delay, an exchange between estimation accuracy and frequency lock–in range results. This paper compares two types of repetition structures with respect to frequency synchronization performance. The *preamble* works with contiguous signal segments and the second exploits repeated signal segments being separated by user data and is called sandwich preamble or *sandamble* [5]. Suitably designed, the latter offers more accuracy and an increased frequency acquisition range. The optimum metric for sandamble detection is derived in [5], [6].

The paper is organized as follows: After the description of transmission model and the two synchronization signal structures in Section II, standard frequency synchronization is reviewed in Section III. In Section IV, we discuss two methods to achieve an extended frequency acquisition range for the sandamble. Analytical results are presented graphically in Section V. The Appendix represents the core of this work and is kept fairly independent from the rest of the paper; it provides the motivation for the lock–in range extension algorithms in Section IV.

This work was supported by Ericsson Eurolab Deutschland GmbH in Nürnberg and is funded in parts by the national research initiative ATMmobil of the German Ministry for Research and Education (BMBF). The author thanks Prof. J. Huber for fruitful discussions.

II. Transmission Model

The discrete–time complex baseband transmit sample of some modulation scheme (e.g., PAM, OFDM) is $s[k]$, where k represents the discrete time. Two training structures are compared, each based on repetition of signal fragments. In the preamble structure shown in Fig. 1a, the training symbols precede the data burst and consist of two identical sample sequences of length D — the first of which starting at discrete–time position $k = 0$. A guard interval of D_g samples is located in time positions $k = -D_\mathrm{g}$ through -1. Those samples are obtained by cyclic repetition of the last D_g samples of the repeated signal segment. Periodicity is symbolized by triangles in Fig. 1. The overall preamble length is $2D + D_\mathrm{g}$. If the channel impulse response is shorter than the guard interval, the correspondence of samples in the intervals $[0, D)$ and $[D, 2D)$ is preserved in the channel–distorted received signal; this periodicity property is exploited for frame- and frequency synchronization in [7].

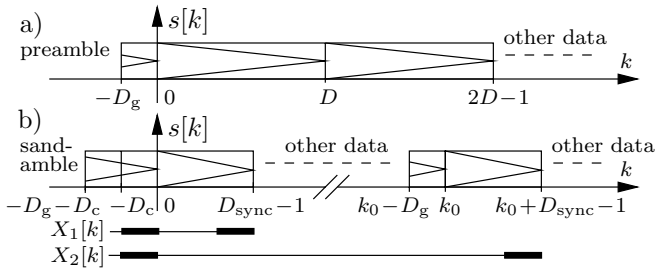

Fig. 1. Transmit signal structure for a) conventional preamble vs. b) proposed sandamble (sandwich preamble) with $D_\mathrm{c} > 0$.

The sandamble in Fig. 1b embeds a payload portion, which is not used for synchronization purposes. The signal parts for synchronization consist of two identical symbol sequences of length D_sync. Their temporal delay is k_0 samples. Now, each segment requires its own guard interval of D_g samples. For the algorithms in Section IV, the first guard interval is eventually extended by another D_c samples. Hence, the overall sandamble length is $2(D_\mathrm{sync}+D_\mathrm{g})+D_\mathrm{c}$. The received burst is usually stored in memory and demodulated off–line, so that the sandamble with embedded data imposes no severe restriction on the system concept. The separation of the repeated signal parts allows a low–variance frequency offset estimation.

The presented algorithms can also be applied in single–

carrier transmission systems, but we consider bursty OFDM. The burst consists of several OFDM symbols, each generated with a D–dimensional inverse discrete Fourier transform (IDFT). For details on OFDM, see [8]. The modulation interval is T and the OFDM subcarrier spacing is $\Delta f_{\text{sub}} = 1/(DT)$.

The repeated signal represents itself an OFDM symbol generated with a D or D_{sync}–dimensional IDFT for preamble or sandamble, respectively. The OFDM symbol could itself carry data, as only the signal repetition property is required for synchronization.

Transmission over the dispersive channel is modelled via channel impulse response $h[k]\,, k = 0, \ldots, D_{\text{e}} - 1$ with excess length D_{e} and $D_{\text{e}} - 1 \leq D_{\text{g}}$. Hence, $s[k]$ is convolved with $h[k]$ to produce the noiseless signal $\tilde{r}_0[k]$. A carrier frequency mismatch is modelled in baseband by modulation with the absolute carrier frequency offset Δf_{co}. This yields the noiseless received sample $\tilde{r}[k] = \tilde{r}_0[k]\,\mathrm{e}^{+\mathrm{j}2\pi\Delta f_{\text{co}}kT} = \tilde{r}_0[k]\,\mathrm{e}^{+\mathrm{j}\frac{2\pi}{D}\xi_f k}$, where we introduced the normalized frequency offset (NFO) $\xi_f \triangleq \frac{\Delta f_{\text{co}}}{\Delta f_{\text{sub}}} = D\Delta f_{\text{co}}T$, which is the frequency offset normalized to the subcarrier spacing of D–point OFDM symbols.

Samples $n[k]$ of additive white Gaussian noise are added to obtain the received sample $r[k] = \tilde{r}[k] + n[k]$.

The average signal power is $\sigma_s^2 \triangleq \mathcal{E}\{|s[k]|^2\} = E_s/T$, where E_s is the average energy per channel symbol. The noise power is $\sigma_n^2 \triangleq \mathcal{E}\{|n[k]|^2\} = N_0/T$, where N_0 is the one–sided power spectral density of the white noise. The channel signal–to–noise power ratio (SNR) at the receiver input is $E_s/N_0 = \sigma_s^2/\sigma_n^2$.

III. Synchronization and its Limits

Optimum frequency estimation [9] performs the (delayed) correlation $S[k] \triangleq \sum_{\kappa=0}^{D_{\text{sync}}-1} r^*[k+\kappa]\,r[k+k_0+\kappa]$, where $D_{\text{sync}} = k_0 = D$ must be used with the preamble. The NFO estimate is $\widehat{\xi_f} = \frac{D}{k_0}\frac{1}{2\pi}\arg(S[\widehat{k}])$, with frame start estimate $\widehat{k}$ obtained from some frame sync stage. Ideally, we have $\widehat{k} = 0$. To increase robustness against wrong frame alignments, the lower and upper sum limits for $S[k]$ could be increased and decreased, respectively.

Note that $\arg(\,\mathrm{e}^{+\mathrm{j}\varphi}) \in (-\pi, \pi]$, $\forall\varphi \in \mathbb{R}$. Owing to the ambiguity of the argument operation for phase values $\pm\pi$ and beyond, the maximum operating range of any such NFO estimator is limited. The nominal upper NFO lock–in range limit is

$$|\xi_f| < D/(2k_0). \tag{1}$$

Obviously, the operating range narrows when the correlation basis k_0 is increased. From now on, we assume for the sandamble the special correlation basis

$$k_0 = D_{\text{sync}} + 2D_{\text{g}} + D, \tag{2}$$

i.e., that exactly one OFDM symbol with its guard interval is embedded by the sandamble. Further, we consider the example parameters

$$D = 64,\ D_{\text{g}} = 8 \text{ and } D_{\text{sync}} = 32 \quad \longrightarrow\ k_0 = 112.$$

With these exemplary system parameters, we obtain $|\xi_f| < 0.286$, which is around half of the lock–in range of the preamble with $|\xi_f| < 0.5$. In the noisy case, the ambiguity limit is not a hard one and we need to calculate ambiguity failure probabilities as function of the NFO.

The quality of the NFO estimate $\widehat{\xi_f}$ is evaluated by its variance in [5] and the sandamble is more power efficient than the preamble. Unfortunately, the NFO acquisition range of the sandamble with $D_{\text{c}} = 0$ might be too small for some applications, so that it needs to be enlarged by $D_{\text{c}} > 0$ exploited by an optimum detection rule [5], [6]. In the following, we concentrate on less complex algorithms to extend the lock–in range.

IV. Lock–In Range Extension for Sandamble

We enlarge the lock–in range via extending the first guard interval by D_{c} samples. Usually, $D_{\text{c}} = 10$ is sufficient such that the sandamble now consists of 90 modulation intervals, representing only approximately 2/3 of the burst overhead of the preamble with 136. One additional correlation with the extended guard interval is

$$X_1[k] \triangleq \sum_{\kappa=1}^{D_{\text{c}}} r^*[k-\kappa]\,r[k+D_{\text{sync}}-\kappa]\,. \tag{3}$$

The position of the correlated signal segments for $X_1[k]$ is indicated by the thickened line portions in Fig. 1b.

For a theoretical understanding of the following algorithms, it is recommended to read Appendix A, first, as there the algorithms are motivated. Note that we have to substitute $D_{\text{c2}} = D_{\text{sync}}$, $\ell_2 = k_0$, $D_{\text{c1}} = D_{\text{c}}$, $\ell_1 = D_{\text{sync}}$, and $\psi_f = 2\pi\xi_f/D$ for mutual correspondence.

A. Coarse/Fine (CF) Approach

This (standard) technique avoids ambiguity prior to fine frequency offset estimation from the argument of $S[k]$. Such a synchronization scheme is described in [2]. A coarse frequency estimate is obtained from $X_1[k]$ in a *pre*processing unit, and the estimated frequency offset is used in the fine estimation based on $S[k]$.

According to Appendix A-A, we obtain the NFO estimate as $\widehat{\xi_f} = \widehat{\xi_f'} + \widehat{\xi_f''}$ with

$$\widehat{\xi_f''} = \frac{D}{D_{\text{sync}}}\frac{1}{2\pi}\arg\left(X_1[\widehat{k}]\right) \text{ and} \tag{4}$$

$$\widehat{\xi_f'} = \frac{D}{k_0}\frac{1}{2\pi}\arg\left(S[\widehat{k}]\,\mathrm{e}^{-\mathrm{j}\frac{2\pi}{D}\widehat{\xi_f''}k_0}\right). \tag{5}$$

The acquisition range limit is $|\xi_f| < D/(2D_{\text{sync}}) = 1$, for our example, and violations occur if the NFO is larger and/or if noise "pulls" $X_1[\widehat{k}]$ or $S[\widehat{k}]$ over the ambiguity boundary.

B. Fine/Discrete (FD) Approach

This newly proposed idea performs a fine estimation of the NFO from $S[k]$ — even though discrete–valued ambiguity may occur —, and finally tries to resolve this ambiguity by a *post*processing discrete detection unit which operates on the appropriately rotated $X_1[k]$. Later, we will mention which advantages are offered by FD when compared to CF.

From Appendix A-C, we now obtain the NFO estimate as $\widehat{\xi_f} = \widehat{\xi_f'} + \frac{D}{k_0}\widehat{\Delta}_f$ with

$$\widehat{\xi_f'} = \frac{D}{k_0}\frac{1}{2\pi}\arg\left(S[\widehat{k}]\right) \quad \text{and} \tag{6}$$

$$\widehat{\Delta_f} = \underset{\tilde{\Delta}_f}{\operatorname{argmax}}\, \Re\left\{X_1[\widehat{k}]\, \mathrm{e}^{-\mathrm{j}\frac{2\pi}{D}\widehat{\xi_f'}D_{\mathrm{sync}}}\, \mathrm{e}^{-\mathrm{j}2\pi\frac{D_{\mathrm{sync}}}{k_0}\tilde{\Delta}_f}\right\}. \tag{7}$$

The fine NFO estimate is limited in range by $-\frac{D}{2k_0} < \xi_f' \leq \frac{D}{2k_0}$, and we can study Fig. 2 for an illustration of the NFO decomposition into discrete intervals with centroid NFOs $\frac{D}{k_0}\Delta_f$ and a continuous–valued fine NFO ξ_f'.

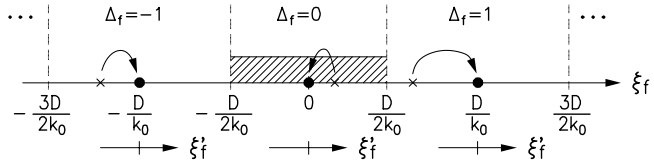

Fig. 2. NFO ambiguity intervals for sandamble. Arrows illustrate the effect of fine "frequency correction"; it "moves" the residual NFO towards interval centroids. If ξ_f lies in the shaded area, no further ambiguity–resolution stage would be required.

From (28), we obtain $\Delta_f^{\max} = \frac{7}{2}$ for our example, indicating that the outermost detectable intervals $\Delta_f = \pm 3$ do *not* coincide. Hence, the maximum acquisition range is $|\xi_f| < \frac{D}{k_0}\Delta_f^{\max} = 2$, which is — in our example — twice as large as that of CF.

Fig. 3 shows the phasor diagram of the expected values of the rotated $X_1[0]$ which correspond with the interval centroid NFOs. Here, only NFO intervals up to $\Delta_f = \pm 2$ are shown. Based on this constellation diagram, the NFO interval detection is performed. Furthermore, it serves as an important tool for the ambiguity failure rate analysis not given in this paper.

To further reduce the detection errors of FD, we can introduce yet another correlation (cf. Fig. 1b for the position of the correlated signal segments)

$$X_2[k] \triangleq \sum_{\kappa=1}^{D_{\mathrm{c}}} r^*[k-\kappa]\, r[k + D_{\mathrm{sync}} + k_0 - \kappa] \tag{8}$$

and replace the discrete detection rule in (7) by the new

$$\widehat{\Delta_f} = \underset{\tilde{\Delta}_f}{\operatorname{argmax}}\, \Re\Big\{\Big(X_1[\widehat{k}]\, \mathrm{e}^{-\mathrm{j}\frac{2\pi}{D}\widehat{\xi_f'}D_{\mathrm{sync}}} + X_2[\widehat{k}]\, \mathrm{e}^{-\mathrm{j}\frac{2\pi}{D}\widehat{\xi_f'}(D_{\mathrm{sync}}+k_0)}\Big)\, \mathrm{e}^{-\mathrm{j}2\pi\frac{D_{\mathrm{sync}}}{k_0}\tilde{\Delta}_f}\Big\}. \tag{9}$$

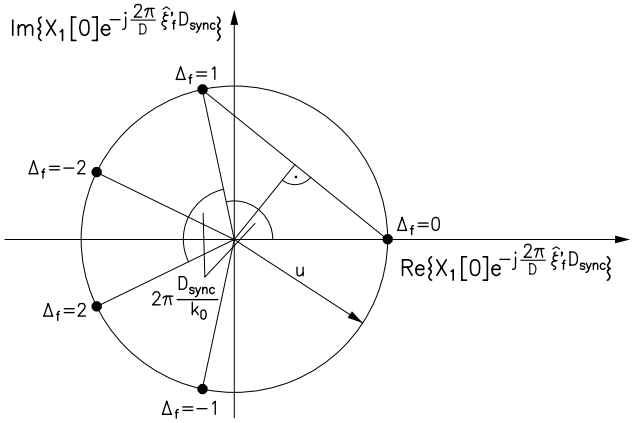

Fig. 3. Phasor diagram of the expected values of the rotated coarse correlation to determine (detect) the number of the ambiguity interval with $|\Delta_f| \leq 2$. The exemplary parameters of the sandamble are $D_{\mathrm{sync}} = 32$ and $k_0 = 112$.

It can be shown that the power efficiency for interval detection is improved by 1.25 dB, if this rotated correlation combining in (9) is employed instead of only $X_1[k]$ in (7). In [5], [6] it is shown that a special weighting of correlation components in (3) and (8) would be optimum because of the joint representation of samples contained in $S[k]$, $X_1[k]$, and $X_2[k]$. This would introduce more complexity, which is not desired in this paper.

V. Power Efficiency of Frequency Estimation

To evaluate the performance of the frequency estimation algorithms, we consider the frequency failure rate $\mathrm{P_{ff}}$ which is defined as the probability that at least one ambiguity limit violation occurred during the $\arg(\cdot)$ operations in the estimation process. As the frequency error usually becomes very large in this case, the data packet can not be demodulated successfully; the burst is lost.

For $\widehat{k} = 0$ in AWGN, all failure rates for the preamble and sandamble can be calculated analytically and due to the length of their derivation, we have to restrict this paper to graphical results, only. In Fig. 4, we show the failure rates $\mathrm{P_{ff}}$ achieved by the preamble, sandamble with CF and sandamble with FD estimating 3 intervals over $|\xi_f|$ for various fairly low SNRs. Often, synchronization must be ensured for SNRs which are still unacceptable for data transmission. For FD, the combining rule according to (9) is always used. The benefit of FD in enlarging the reliable fraction of the lock–in range is dramatical up to $|\xi_f| \approx 0.8$, where FD outperforms CF. For CF, the gradual degradation begins already at $|\xi_f| = 0.714$. The preamble offers only a small nominal acquisition range of $|\xi_f| < 0.5$, further "reduced" by the noise influence. In contrast to the sandamble *with* extended lock–in range, no error floor occurs for the preamble at lower NFOs.

Fig. 5 presents results for an FD algorithm with 5 intervals in AWGN and we see that now FD offers by far

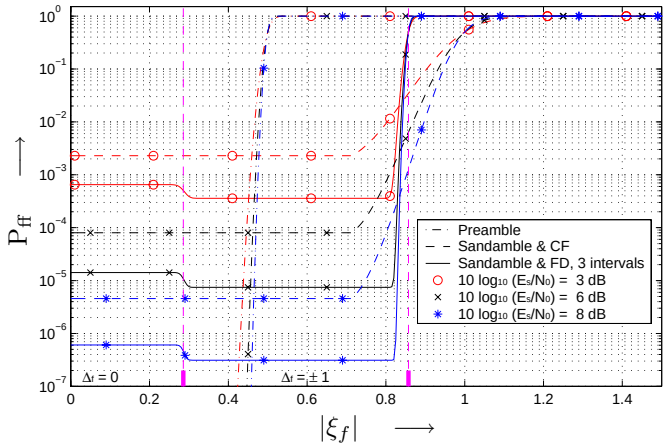

Fig. 4. Frequency estimation failure rate vs. NFO for preamble, sandamble & CF, and sandamble & FD with 3 intervals in AWGN for $\widehat{k} = 0$. The guard interval extension is $D_c = 10$.

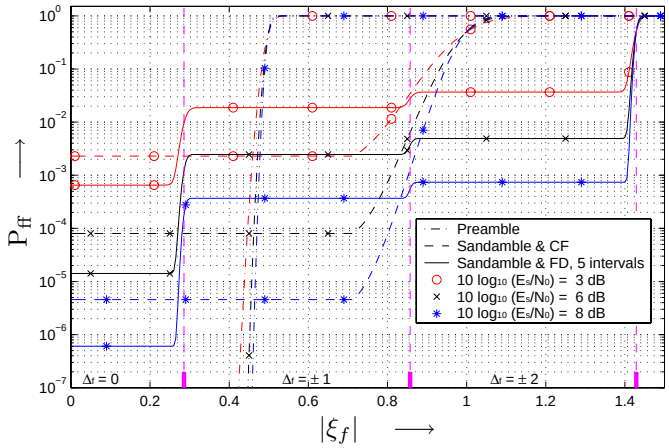

Fig. 5. Frequency estimation failure rate vs. NFO for preamble, sandamble & CF, and sandamble & FD with 5 intervals in AWGN for $\widehat{k} = 0$. The guard interval extension is $D_c = 10$.

the largest frequency acquisition range in exchange with power efficiency inside the acquisition range. From Fig. 3, we see that the formerly robust detection of the intervals $\Delta_f = \pm 1$ now suffers from the proximity of the "constellation points" for $\Delta_f = \pm 2$, which leads to an increased P_{ff} in the intervals ± 1. If we consider a non–uniform pdf for ξ_f with a maximum at NFOs around zero (e.g., Gaussian pdf, triangular[1] pdf), then we may conclude that FD with these system parameters is unbeatable due to its very good performance for the highly probable near–zero NFOs and increasingly worse performance for the higher NFOs which occur rarely.

VI. Summary and Conclusions

We presented the performance of a sandwich repetition preamble (sandamble) scheme in comparison to a standard repetition preamble. We outlined the advantage of the sandamble in terms of burst overhead vs. NFO estimation accuracy. Further, we considered the easily implementable CF and FD strategies to extend the limited lock–in range of the sandamble by exploiting additional unweighted correlations. The FD approach outperforms CF for a wide variety of parameters.

The single–shot frequency failure rate of FD seems to be acceptable in burst mode transmission systems and could be further reduced by enlarging the correlation diversity D_c or by introducing memory into the NFO interval decision rule. This requires storage of the estimated NFO from previous bursts and exploiting this knowledge in the current decision. Given the fact, that the NFO is not jumping in large steps, the interval decisions can be "smoothed" on the basis of several bursts, such that interval misestimations become very rare due to the uncorrelatedness of the noise in the single bursts. The sandamble structure in combination with the FD estimation strategy for ambiguity resolution (lock–in range extension) offers immense flexibility to trade lock–in range against estimation robustness and burst overhead for synchronization. Even an adaptive receiver mode is feasible which adapts to the oscillator quality or switches between some kind of acquisition and tracking mode.

Appendix

A. Frequency Estimation Using Two Correlation Results

This appendix is kept independent from specific parameters. We compare three frequency estimation strategies with extended lock–in range which all rely on the observation of two correlations with differing parameters.

We assume availability of two correlation results $L_\nu \triangleq \sum_{\kappa=0}^{D_{c\nu}-1} r^*[K_\nu + \kappa]\, r[K_\nu + \ell_\nu + \kappa]$, $\nu = 1, 2$, where we denote the *correlation basis* (distance of correlated samples) with ℓ_ν and the *correlation diversity* (number of exploited sample pairs) with $D_{c\nu}$. We restrict our analysis to $D_{c\nu} \le \ell_\nu$. In contrast to the actualities with the sandamble, the time offsets K_1 and K_2 are assumed to be different and chosen such that none of the samples used for L_1 is exploited for L_2. A further assumption is $\ell_1 < \ell_2$ and $D_{c1} < D_{c2}$, reflecting dominance of L_2.

For the noiseless received samples, we require the signal periodicity property $\tilde{r}[K_\nu + \ell_\nu + \kappa] = \mathrm{e}^{+\mathrm{j}\psi_f \ell_\nu} \tilde{r}[K_\nu + \kappa]$, $0 \le \kappa \le D_{c\nu} - 1$, $\nu = 1, 2$, where ψ_f is the normalized phase velocity (NPV). Clearly, this periodicity needs to be introduced into the signal to serve for our frequency estimation purposes. With a carrier frequency offset, we have $\psi_f = 2\pi \Delta f_{co} T$, with T being the modulation interval and Δf_{co} the absolute carrier frequency offset.

Further, we need to introduce the (random) variables

[1] If we assume an uniform pdf for the uncorrelated oscillator frequency offsets in transmitter and receiver, respectively, then the pdf of the NFO is triangular.

$u_\nu = \frac{1}{\sigma_s^2}\sum_{\kappa=0}^{D_{c\nu}-1}|\tilde{r}[K_\nu+\kappa]|^2$, $\nu = 1,2$, which represent the normalized noiseless correlation magnitudes being identical with the energy sum in one of the repeated signal segments. The average power of $\tilde{r}[k]$ is σ_s^2 and if the samples $\tilde{r}[K_\nu+\kappa]$ origin from constant–energy single–carrier modulation transmitted over a non–dispersive channel, then we have the constant $u_\nu = D_{c\nu}$. If the correlated samples represent an OFDM signal *fragment*, then u_ν is a random variable which approximates a central chi–square distribution with $2D_{c\nu}$ degrees of freedom.

The conditional mean value of the correlations is

$$\mathcal{E}\{L_\nu|u_\nu,\psi_f\} = u_\nu\sigma_s^2\ \mathrm{e}^{+\mathrm{j}\psi_f\ell_\nu}. \tag{10}$$

Note, the correspondence of L_1 and L_2 with the little and the big hand of a watch, respectively; while L_2 makes one full rotation for a specific NPV, then L_1 manages only a fraction of ℓ_1/ℓ_2 of a full circle.

A. Coarse/Fine Approach

The obvious brute forward solution for NPV estimation based on the two correlations L_1 and L_2 is to exploit the correlation with the smallest correlation basis, i.e., L_1, to obtain a **coarse** (initial) estimate for the NPV by

$$\widehat{\psi_f''} = \frac{1}{\ell_1}\arg(L_1). \tag{11}$$

Clearly, this first estimation will not be perfect and we introduce the residual NPV (estimation error)

$$\psi_f' = \psi_f - \widehat{\psi_f''}. \tag{12}$$

Now, we can perform the **fine** estimation of the residual NPV from L_2 by

$$\widehat{\psi_f'} = \frac{1}{\ell_2}\arg\left(L_2\,\mathrm{e}^{-\mathrm{j}\widehat{\psi_f''}\ell_2}\right). \tag{13}$$

The final NPV estimate is

$$\widehat{\psi_f} = \widehat{\psi_f'} + \widehat{\psi_f''} \tag{14}$$

and it is clear that successful overall estimation results iff the $\pm\pi$ ambiguity boundary of the $\arg(\cdot)$ operation is not violated in none of both phase estimation processes.

With the CF algorithm the lock–in range is always upper bounded by $|\psi_f| < 2\pi/(2\ell_1)$.

B. Maximum–Likelihood Approach

We need to assume that the effective noise in L_ν is Gaussian[2] distributed with the conditional mean according to (10) and conditional variance $\mathcal{E}\{|L_\nu-\tilde{L}_\nu|^2\ |\ u_\nu\} = 2u_\nu\sigma_s^2\sigma_n^2 + D_{c\nu}\sigma_n^4$ such that we have the conditional pdf

$$\begin{aligned} p_{L_\nu}(L_\nu|u_\nu,\psi_f) &\sim \exp\left(-\frac{\left|L_\nu - u_\nu\sigma_s^2\cdot\mathrm{e}^{+\mathrm{j}\psi_f\ell_\nu}\right|^2}{2u_\nu\sigma_s^2\sigma_n^2 + D_{c\nu}\sigma_n^4}\right) \\ &\sim \exp\left(\frac{\Re\{L_\nu\,\mathrm{e}^{-\mathrm{j}\psi_f\ell_\nu}\}}{\sigma_n^2\left(1+\frac{D_{c\nu}}{2u_\nu E_s/N_0}\right)}\right). \end{aligned} \tag{15}$$

Now we perform a medium to high SNR approximation of the pdf and obtain

$$p_{L_\nu}(L_\nu|u_\nu,\psi_f) \sim \exp\left(\frac{1}{\sigma_n^2}\Re\{L_\nu\,\mathrm{e}^{-\mathrm{j}\psi_f\ell_\nu}\}\right). \tag{16}$$

Exploiting that noise in the correlation results L_1 and L_2 is uncorrelated, the joint pdf can be approximated as

$$\begin{aligned} &p_{L_1,L_2}(L_1,L_2|u_1,u_2,\psi_f) \\ &\quad\sim \exp\left(\frac{1}{\sigma_n^2}\Re\{L_1\,\mathrm{e}^{-\mathrm{j}\psi_f\ell_1} + L_2\,\mathrm{e}^{-\mathrm{j}\psi_f\ell_2}\}\right). \end{aligned} \tag{17}$$

We emphasize again that this is not true in the sandamble structure from the main section, but we assume uncorrelatedness in this appendix. Hence, the high–SNR maximum–likelihood (ML) estimate of the NPV can be found by

$$\widehat{\psi_f} = \underset{\tilde{\psi}_f}{\operatorname{argmax}}\ \Re\left\{L_1\,\mathrm{e}^{-\mathrm{j}\tilde{\psi}_f\ell_1} + L_2\,\mathrm{e}^{-\mathrm{j}\tilde{\psi}_f\ell_2}\right\}, \tag{18}$$

which needs to be evaluated by an exhaustive search over the desired lock–in range or an iterative maximum search (e.g., Newton iteration). Often this optimum[3] procedure is prohibitive due to complexity or limited processing time resources in the receiver.

We mention the theoretically achievable maximum lock–in range to be $|\psi_f| < \psi_f^{\max}$ with

$$\psi_f^{\max} = \tfrac{1}{2}\ \min\left(\left\{\psi_f\in\mathbb{R}^+\middle|\ \tfrac{\ell_1}{2\pi}\psi_f\in\mathbb{Z}\bigwedge\tfrac{\ell_2}{2\pi}\psi_f\in\mathbb{Z}\right\}\right) \tag{19}$$

and it is obvious that the lock–in range can be made very large as long as ℓ_1 and ℓ_2 are sufficiently prime. In other words: To achieve a very large acquisition range (at the expense of power efficiency) for frequency synchronization with the help of two correlations, the correlation basis ℓ_2 should *not* be a multiple of ℓ_1.

C. Fine/Discrete Approach

This approach is based on the near–ML estimation rule (18). Here, we assume the NPV to be composed of a discrete and a fractional part such that we have

$$\psi_f = \psi_f' + \frac{2\pi}{\ell_2}\Delta_f\,,\ -\frac{\pi}{\ell_2} < \psi_f' \le \frac{\pi}{\ell_2} \text{ and } \Delta_f\in\mathbb{Z}. \tag{20}$$

[2]The overall noise in the correlation result L_ν is composed of two components which are different in nature. The noise–signal component is two times the sum of Gaussian noise samples scaled by the useful signal samples and therefore its conditional pdf is Gaussian. The noise–noise component is the sum of $D_{c\nu}$ products of pairs of Gaussian noise samples and, clear enough, each of these single products is not Gaussian distributed. Via the central limit theorem their sum can be approximated as nearly Gaussian.

[3]If ψ_f is non–uniformly distributed in the search interval, then a maximum a–posteriori estimation rule would be optimum which considers the a–priori pdf of ψ_f. Due to the increased complexity (and usually moderate gains) this possibility is not considered here.

We study the mean values of the correlations from (10) under this assumption and we obtain

$$\mathcal{E}\{L_1 \big| u_1, \psi'_f, \Delta_f\} = u_1 \sigma_s^2 \, \mathrm{e}^{+\mathrm{j}\left(\psi'_f \ell_1 + 2\pi \frac{\ell_1}{\ell_2} \Delta_f\right)} \tag{21}$$

$$\mathcal{E}\{L_2 \big| u_2, \psi'_f, \Delta_f\} = u_2 \sigma_s^2 \, \mathrm{e}^{+\mathrm{j}\psi'_f \ell_2} = \mathcal{E}\{L_2 \big| u_2, \psi'_f\}. \tag{22}$$

Obviously, the expected value of L_2 does not depend on Δ_f. Note that an estimate of Δ_f can only be obtained from L_1 iff the ratio of ℓ_1 and ℓ_2 is appropriately designed. With these expected values, the high–SNR ML estimate of the NPV from (18) becomes

$$\{\widehat{\psi'_f}, \widehat{\Delta}_f\} = \underset{\{\tilde{\psi}'_f, \tilde{\Delta}_f\}}{\operatorname{argmax}} \, \Re\Big\{ L_1 \, \mathrm{e}^{-\mathrm{j}\tilde{\psi}'_f \ell_1} \, \mathrm{e}^{-\mathrm{j}2\pi \frac{\ell_1}{\ell_2} \tilde{\Delta}_f} + L_2 \, \mathrm{e}^{-\mathrm{j}\tilde{\psi}'_f \ell_2} \Big\} \tag{23}$$

and up to this point no further approximation has been used. For a still optimum performance, a joint exhaustive search over the reduced continuous–valued range of $\tilde{\psi}'_f$ and the discrete $\tilde{\Delta}_f$ needs to be done. This already offers some implementational advantage over the full search given in (18).

Now, we make use of the fact that $|\mathcal{E}\{L_2\}| > |\mathcal{E}\{L_1\}|$ which is valid due to $D_{\mathrm{c}2} > D_{\mathrm{c}1}$, i.e., the dominance of L_2. Owing to this higher significance of L_2 we approximate the original two-dimensional estimation process by splitting it up into two one–dimensional processes of **fine** estimation and **discrete** detection

$$\widehat{\psi'_f} = \underset{\tilde{\psi}'_f}{\operatorname{argmax}} \, \Re\Big\{ L_2 \, \mathrm{e}^{-\mathrm{j}\tilde{\psi}'_f \ell_2} \Big\} = \frac{1}{\ell_2} \arg(L_2) \tag{24}$$

$$\widehat{\Delta_f} = \underset{\tilde{\Delta}_f}{\operatorname{argmax}} \, \Re\Big\{ L_1 \, \mathrm{e}^{-\mathrm{j}\widehat{\psi'_f} \ell_1} \, \mathrm{e}^{-\mathrm{j}2\pi \frac{\ell_1}{\ell_2} \tilde{\Delta}_f} \Big\}. \tag{25}$$

The fractional NPV $\widehat{\psi'_f}$ and the NPV interval number $\widehat{\Delta_f}$ are determined separately, but the estimate ("decision") from the first step is used in the second such that a feedback or "multistage" estimation structure results.

For the rotated L_1, we find (cf. Eq. (21))

$$\mathcal{E}\{L_1 \, \mathrm{e}^{-\mathrm{j}\widehat{\psi'_f} \ell_1} \big| u_1, \Delta_f\} = u_1 \sigma_s^2 \, \mathrm{e}^{+\mathrm{j}2\pi \frac{\ell_1}{\ell_2} \Delta_f} \tag{26}$$

due to the fact that $\widehat{\psi'_f}$ is an unbiased estimate of ψ'_f. Furthermore, $\widehat{\psi'_f}$ will be a low–variance (i.e., quite exact) estimate, as we have $\ell_2 > \ell_1$ and $D_{\mathrm{c}2} > D_{\mathrm{c}1}$. Thus, the rotation of L_1 according to the estimate $\widehat{\psi'_f}$ is very reliable and can be assumed to be near–perfect. The expected values in (26) represent discrete points with defined phase angles on a circle, which can be interpreted as a general "constellation" diagram.

The final NPV estimate is

$$\widehat{\psi_f} = \widehat{\psi'_f} + \frac{2\pi}{\ell_2} \widehat{\Delta}_f, \tag{27}$$

and it exhibits nearly the same performance as the optimum rule in (18) as long as the dominance of L_2 is valid.

With the FD algorithm, the lock–in range can be quite large and it is upper bounded by $|\psi_f| < \frac{2\pi}{\ell_2} \Delta_f^{\max}$ with

$$\Delta_f^{\max} = \tfrac{1}{2} \, \min\Big(\{ \Delta_f \in \mathbb{Z}^+ \big| \, \tfrac{\ell_1}{\ell_2} \Delta_f \in \mathbb{Z} \} \Big). \tag{28}$$

Again, it is obvious from (28) that ℓ_1 and ℓ_2 should be relatively prime (at least no simple multiples of each other) if a large lock–in range is desired. Note that $\Delta_f^{\max}$ can become non–integer, indicating that the outermost detectable intervals $\pm\lfloor \Delta_f^{\max} \rfloor$ do *not* coincide and need not to be separated by a third step. If $\Delta_f^{\max} \in \mathbb{Z}$ then the intervals $\pm\Delta_f^{\max}$ do coincide and the NPV estimate ambiguity requires the sign of $\widehat{\psi'_f}$ to be further resolved. This is due to the fact that the combination $|\widehat{\Delta}_f| = \Delta_f^{\max}$ and $\operatorname{sign} \widehat{\psi'_f} < 0$ represents a positive NPV, while $|\widehat{\Delta}_f| = \Delta_f^{\max}$ and $\operatorname{sign} \widehat{\psi'_f} > 0$ indicates a negative NPV. The final improved NPV estimation rule accounting for $\Delta_f^{\max} \in \mathbb{Z}$ is

$$\widehat{\psi_f} = \begin{cases} \widehat{\psi'_f} - \frac{2\pi}{\ell_2} \Delta_f^{\max} \operatorname{sign} \widehat{\psi'_f} & |\widehat{\Delta}_f| = \Delta_f^{\max} \\ \widehat{\psi'_f} + \frac{2\pi}{\ell_2} \widehat{\Delta}_f & |\widehat{\Delta}_f| < \Delta_f^{\max} \end{cases}. \tag{29}$$

References

[1] Paul H. Moose, "A Technique for Orthogonal Frequency Division Multiplexing Frequency Offset Correction," *IEEE Trans. on Commun.*, vol. 42, no. 10, pp. 2908–2914, 1994.

[2] Uwe Lambrette, Michael Speth, and Heinrich Meyr, "OFDM Burst Frequency Synchronization by Single Carrier Training Data," *IEEE Communications Letters*, vol. 1, no. 2, pp. 46–48, 1997.

[3] Andreas Czylwik, "Synchronisation für Einträgerübertragung mit Entzerrung im Frequenzbereich und geringen Kapazitätsverlusten durch Pilot–Symbole (in German)," in *3. OFDM–Fachgespräch*, Braunschweig, Germany, September 1998.

[4] Stefan Müller–Weinfurtner, "On the Optimality of Metrics for Coarse Frame Synchronization in OFDM: A Comparison," in *Proceedings of IEEE International Symposium on Personal, Indoor and Mobile Radio Communications (PIMRC'98)*, Boston, Mass., USA, September 1998, pp. 533–537.

[5] Stefan Müller–Weinfurtner, "Sandwich Preamble for Burst Synchronization," in *Proceedings of 5th International OFDM–Workshop 2000*, Hamburg, Germany, September 2000, pp. 23.1–23.4.

[6] Stefan Müller–Weinfurtner, *OFDM for Wireless Communications: Nyquist Windowing, Peak–Power Reduction, and Synchronization*, Reihe Kommunikations- und Informationstechnik, Band 16, ISBN 3-8265-7658-6. Shaker Verlag, Aachen, 2000, Dissertation Universität Erlangen–Nürnberg.

[7] Pierre R. Chevillat, Dietrich Maiwald, and Gottfried Ungerboeck, "Rapid Training of a Voiceband Data–Modem Receiver Employing an Equalizer with Fractional–T Spaced Coefficients," *IEEE Trans. on Commun.*, vol. 35, no. 9, pp. 869–876, 1987.

[8] Hikmet Sari, Georges Karam, and Isabelle Jeanclaude, "Transmission Techniques for Digital Terrestrial TV Broadcasting," *IEEE Communications Magazine*, vol. 33, no. 2, pp. 100–109, 1995.

[9] Jan-Jaap van de Beek, Magnus Sandell, and Per Ola Börjesson, "ML Estimation of Time and Frequency Offset in OFDM Systems," *IEEE Transactions on Signal Processing*, vol. 45, no. 7, pp. 1800–1805, 1997.